FDC Progress Report (September 2006)

Simon Taylor
Ohio University

Daniel S. Carman
Jefferson Lab and Ohio University

David Lawrence
Jefferson Lab

Brian Kross
Jefferson Lab

September 28, 2006

Abstract

This report details progress toward the design of a full-scale prototype cathode chamber for the FDC system of the GlueX experiment in Hall D at Jefferson Lab. This work is based on studies of a small-scale prototype that has been under test and an ongoing R&D program in conjunction with the Jefferson Lab Detector Group. The design of the full-scale prototype is based on lessons learned from the small-scale detector and the R&D program with an aim to identify and to mitigate all risk areas.

1 Forward Drift Chamber System

The Forward Drift Chamber (FDC) system in the GlueX detector in Hall D at Jefferson Lab (JLab) consists of a set of 24 planar drift chambers with cathode readout that is grouped into four identical disk-shaped packages of six chambers. This system is designed to track forward-going particles from the target ($2^\circ < \theta < 20^\circ$) in the 2 T magnetic field of the GlueX solenoid. A schematic picture of a single FDC package is shown in Fig. 1. Details on the FDC prototype studies and design work is contained on the FDC web page [1]. Fig. 2 shows the position of the FDC packages within the full GlueX detector.

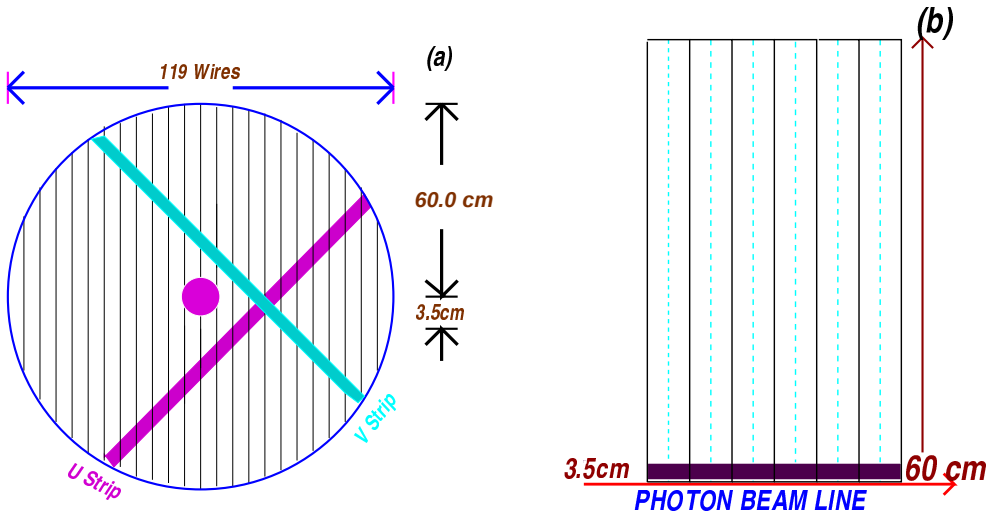

Figure 1: A front (a) and side (b) sketch of an FDC package. In (a) the wires are schematically indicated as the vertical lines. The U cathode strips are in front of the wires and the V cathode strips are behind the wires. In (b) is shown a side view of the upper half of a six-chamber package. The wire planes are shown as the dashed lines, while the cathode planes are shown as the solid lines. Ground planes between adjacent chambers are not shown.

Each chamber is 1.2 m in diameter and consists of a wire plane flanked on either side by cathode planes divided into thin strips as illustrated in Fig. 3. The strips are oriented at $\pm 45^\circ$ with respect to the wires and 90° with respect to each other. Neighboring chamber layers will be rotated by 60° with respect to each other in order to improve track reconstruction decisions on the corresponding left/right ambiguities in the wire planes, hence improving the overall resolution. By charge interpolation of the electron avalanche image charge in the cathode strip readout, spatial resolutions at the cathode planes are expected of better than 200 μm. The purpose of crossing the strips is to provide redundant coordinate information, as well as to aid in pattern recognition in the background environment expected in the GlueX detector (see Section 2). The individual hits from each of the packages will then be linked via the analysis software to reconstruct the spiraling tracks in the GlueX solenoidal magnetic field. The nominal design parameters for the FDC detector system are given in Appendix I.

The primary development issues associated with the FDCs that must be addressed are factors affecting the intrinsic resolution of the chambers, along with the mechanical and electronics layout. The goal is to construct a tracking detector that meets the required

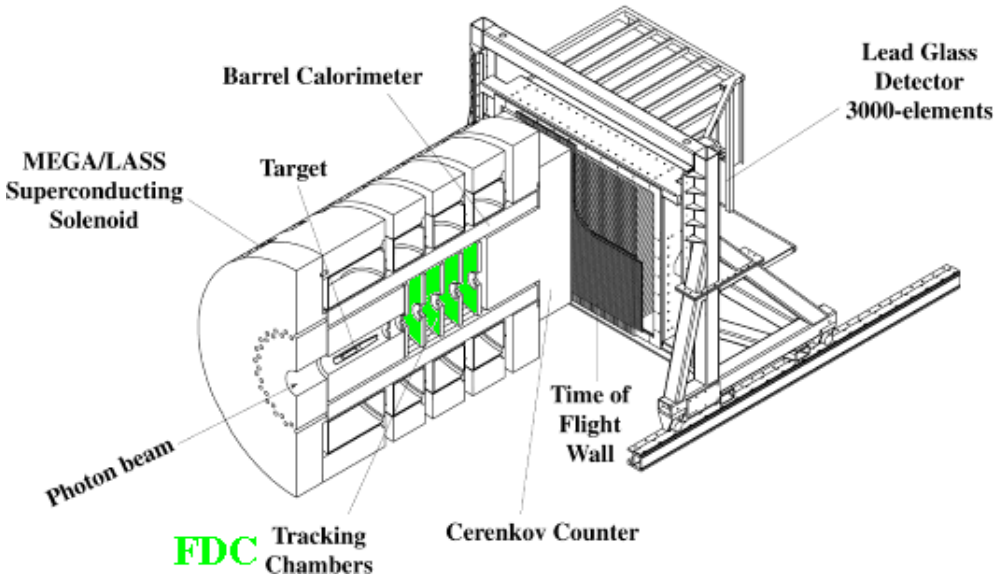

Figure 2: A schematic picture of the GlueX detector showing the location of the four FDC packages within the solenoid magnet.

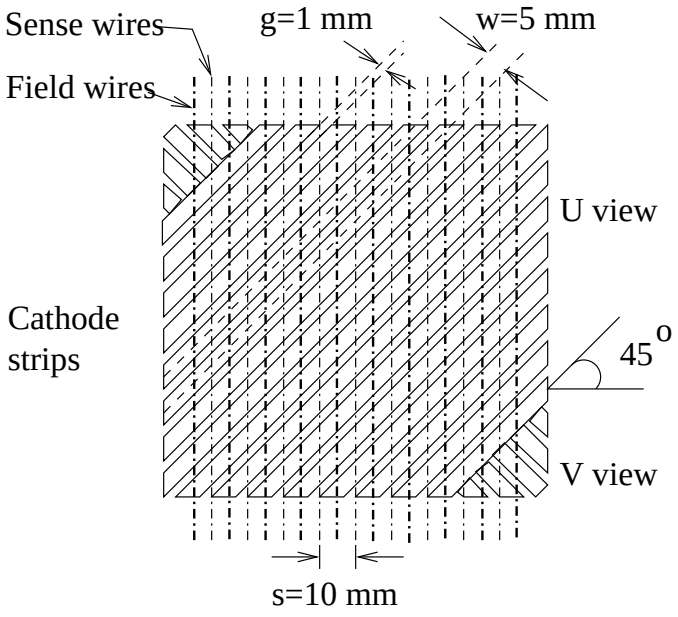

Figure 3: Schematic drawing of the orientation of the cathode strips flanking a given wire plane. The strip pitch w=5 mm and the strip-to-strip gap g=1 mm. The sense wire separation s=10 mm. The two cathode readout views are referred to as U and V.

design specifications and has a long life time, a uniform and predictable response, a high efficiency, and is serviceable in case of component failure.

1.1 FDC Design Details

Each wire plane consists of alternating field and sense wires, with a sense to field wire separation of 5 mm and a wire plane to cathode plane separation of 5 mm. The nominal design for the cathode planes calls for a strip pitch of 5 mm and a strip-to-strip separation of 1 mm (see Fig. 4. The strips will lay on a 2-mil thick Kapton backing. The strips themselves will be copper with a thickness of 0.25 oz. Studies of our small-scale prototype with copper layers of two thicknesses (1.0 oz and 0.25 oz) have been carried out and the 0.25 oz option is the thinnest copper layer that allows for signal integrity above our specifications. Minimization of the overall chamber thickness is important to reduce multiple scattering and energy loss. A ground plane is included between neighboring cathode planes to ensure minimal signal cross-talk.

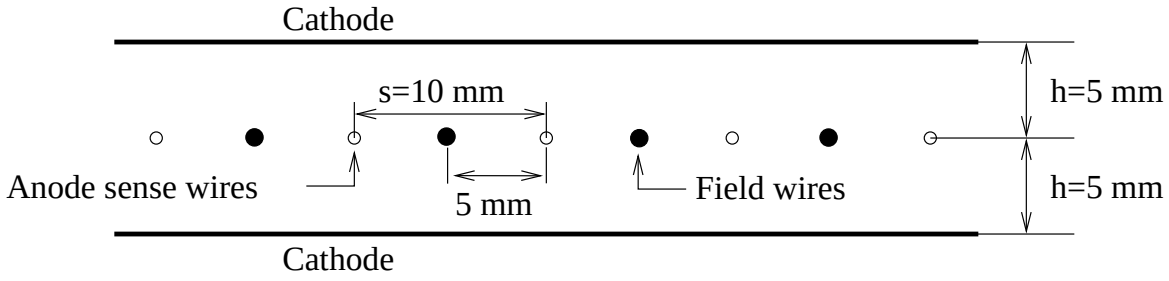

Figure 4: Schematic end view (wires projecting into and out of the plane of the page) defining the nominal electrode geometry of the FDC system

To limit wire tensions and operating voltages implies that the wire diameter has to be minimized. The anode wire for the chambers will consist of 20-μm diameter gold-plated tungsten, the smallest practical choice. Tungsten is a good choice because of its durability, and the gold-plating of the wires ensures chemical inertness as well as a smooth surface finish. The expected electronics gain and thresholds dictate that the gas gain be a few times 10^4. Under this condition, the electric field at the surface of the sense wires is $\approx$280 kV/cm. The field-wire diameter is chosen to ensure that the electric field at their surface remains below 20 kV/cm to minimize conditions causing cathode deposits [2, 3]. The field wire diameter will be chosen to be 100 μm. Gold-plated aluminum is a good choice because it has the longest radiation length of any practical wire material and thus minimizes multiple scattering. Additionally, the low density of aluminum means that the field wires can be strung at lower tension than a more dense wire, with minimal gravitational sag. This minimizes the forces on the support frames. Presently we are seeking out vendors to supply the wire for the chambers that will meet our tolerances and specifications. We will rely on our experiences from construction of the drift chambers in Hall B to make the final vendor selection.

The wires that cross through the beam line require special treatment to handle the otherwise unmanageable rates. Several possibilities are currently being considered. The first is to deaden the wires out to a radius of $\sim$3.5 cm by placing a material such as Styrofoam

around them. Another attractive alternative that has been perfected at Fermilab [4] is to deposit a layer of metal on that portion of the wires to be deadened to build up the wire diameter. This technique then reduces the surface electric field on this portion of the wire to the point where the gain is reduced below the level necessary for the electron avalanche to be formed.

1.2 Readout

The readout of the full set of FDC detectors will require on the order of 2850 anode (sense wire) channels and 11400 cathode channels. The exact numbers are subject to the details of the mechanical design, which is presently underway. The signals will be amplified at the detector using an 8-channel ASIC preamplifier/shaper chip based on the ASDBLR ASIC used to readout the ATLAS-TRT (see Fig. 5). The pulse shape will be chosen as a compromise between noise and pileup, both of which degrade the resolution. The electronics must also be designed to minimize cross-talk, particularly to non-adjacent channels. The design of this component is the responsibility of the University of Alberta and the University of Pennsylvania.

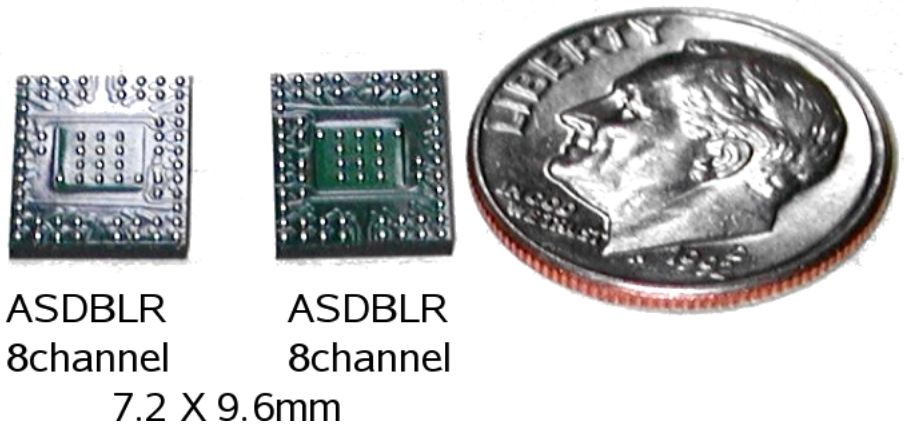

Figure 5: Photographs of two ASDBLR ASICs used in the ATLAS-TRT detector.

The nominal data acquisition plan calls for the cathode strips to be read out with commercially available 100 MHz flash ADCs and the anode wires to be read out with commercially available F1 TDCs. We are also investigating an alternative approach in which we would use flash ADCs to read out the anode wires as well as the cathode strips. In our small-scale prototype, we are employing the same preamplifiers as used for the CLAS drift chambers, as the ASIC chips for GlueX are not yet ready for detector testing, but our readout electronics employ the flash ADCs and TDCs expected to be used for the final GlueX FDC readout.

The 100 MHz flash ADCs that will be employed for the cathode readout have a sampling rate that corresponds to a 10.0 ns time bin. Time fitting algorithms matched to the chamber pulse shape can be employed to provide a time resolution of $\sim$2 ns (amounting to $\sim$20% of the time bin width). This timing information from the cathode signals will significantly aid in resolving hits from multiple tracks passing through the chamber volume.

The primary design issue for the front-end electronics for the FDC system is to maintain a signal-to-noise ratio of better than 100:1 in the presence of a large detector capacitance.

Capacitance measurements in detectors are very important because they serve to determine the performance of the detector in terms of the charges induced on the cathodes, gain variations, detector efficiency, etc. They also play an important role in determining the characteristics of the readout electronics. For the FDC chambers the dominant contribution to the capacitance seen by the preamplifiers will be the strip-to-strip capacitance. The capacitance between adjacent strips is given approximately by [5]:

$$C(pF/cm) = 0.12t/w + 0.09(1+k)log_{10}(1 + 2w/s + w^2/s^2), \quad (1)$$

where t is the strip thickness, w is the strip width, s is the strip separation, and k is the dielectric constant of the backing material (here it is envisioned to be kapton). For the FDC design that is presently considered, this capacitance is roughly 1 pF/cm. Accounting for the total capacitance of the system then forms a basic requirement for the input capacitance for the front-end electronics performance. An additional concern for this design is the coupling of the signals between adjacent strips. Studies of the PHENIX CSCs have shown that appropriate setting of the integration times of the electronics is important to decrease sensitivity to distortions in the induced charge distribution due to inter-strip coupling.

1.3 Resolution Effects

Resolution degradation of cathode chambers comes primarily from two sources, tracks inclined from the normal to the face of the chamber and Lorentz angle effects. In both cases the spatial resolution is degraded because the avalanche charge is distributed non-uniformly along the anode wire due to the energy loss fluctuations in the gas. The cathode position resolution is optimum when the avalanche is formed at a single point along the wire. A finite spatial extent of the anode charge results in a resolution degradation $\mathcal{D}$. Studies of the PHENIX cathode chamber [5] have shown that $\mathcal{D}$ goes as:

$$\mathcal{D} = 0.16d\tan\theta, \quad (2)$$

where d is the anode-to-cathode spacing and θ is the angle from the normal to the face of the chamber.

Skewed or non-local charge distributions along the anode wire can also be caused by a Lorentz force along the anode wire from the presence of magnetic field components that are not collinear with the electric field of the chambers. The Lorentz effect itself does not result in a systematic shift of the measured coordinate in the cathode plane. It simply results in a degradation of the resolution because of the spread of the charge along the wire.

1.4 Gas Considerations

There are several basic requirements that need to be met by the chamber gas that will be used for the FDC system. These include a high drift velocity (50-60 μm/ns), low Lorentz angle ($< 10^\circ$), and for safety, we much prefer a non-flammable mixture. It is important to understand that the performance of a cathode chamber in terms of cathode position resolution is reasonably insensitive to the exact values of the gas parameters. Here variations of the drift velocity or non-uniform drift velocities as a function of E/p (i.e. electric field/pressure)

are relatively unimportant. For the same reason, the cathode readout operation is immune to modest variations of temperature and pressure. Variations in gas gain on the order of 20% do not strongly affect the cathode resolution since a relative charge measurement in adjacent strips is involved.

However, the gas mixture and its control are essential to consider carefully for the operation of the MWDC. In order to enable accurate calibrations of the drift times, it is essential that the gas mixture is stable, which amounts to constructing a gas handling system that carefully controls the gas mixture, as well as hall controls to fix the temperature and relative humidity as much as possible. A gas system for the FDC prototype is currently under design by Brian Kross of the JLab Detector Group.

Detailed studies of chamber performance will be performed with our prototype cathode chamber employing various gas mixtures. A number of gas mixtures have been studied by various groups that have proven suitable for cathode chambers. Most of these gases contain CF_4 in combination with isobutane (C_4H_{10}) or CO_2. The Lorentz angle is similar for each gas and is about 5° at 0.5 T magnetic field. One chamber-safe gas mixture that has worked well with the PHENIX cathode chambers consists of 30% argon, 50% CO_2, and 20% CF_4.

2 Cathode Chambers

Cathode chambers are not a new technology to nuclear and particle physics experiments, and many of the design choices in the construction of the small-scale prototype were based on existing designs. The small-scale FDC prototype chamber has the same electrode configuration as planned for the full-scale prototype, but is square in design with an active area of 20 cm × 20 cm (see Section 3).

Cathode strip chambers (CSC) are typically multiwire proportional chambers (MWPCs) with a symmetric drift cell in which the anode-cathode spacing d is equal to the anode wire pitch s (see Fig. 6). In these chambers the spatial resolution of the anode readout is limited to roughly $s/\sqrt{12}$ (RMS). In a CSC the precision coordinate is obtained by measuring the charge induced on a segmented cathode by the electron avalanche formed on the anode wire as shown in Fig. 7. However, CSCs can also be used to measure a three dimensional space point on a track by rotating the opposing cathode plane strips at an angle with respect to each other. For the case of multiple tracks, a second segmented cathode can also help to reduce multi-hit ambiguities as shown in Fig. 8. The stereo technique is superior to the alternative of reading out only one cathode plane and a hit wire number in that multiple hits on a single wire may be resolved.

The optimum cathode readout pitch w is determined by the width of the induced charge distribution. It has been shown by several groups that minimal differential non-linearity (∼1%) is achieved when $w/d \approx 1$ (e.g. [6]). This ratio is employed in the current FDC design.

Simulations from Ref. [6] have shown that resolutions of 25 μm could be achieved for minimum-ionizing tracks if the electronics and readout could be provided with noise and inter-channel gain variations of less than 0.5% of the nominal pulse height. The primary factor limiting the spatial resolution of a cathode chamber is the electronic noise of the preamplifier. Other factors such as the uncertainty in the gain calibrations and cathode

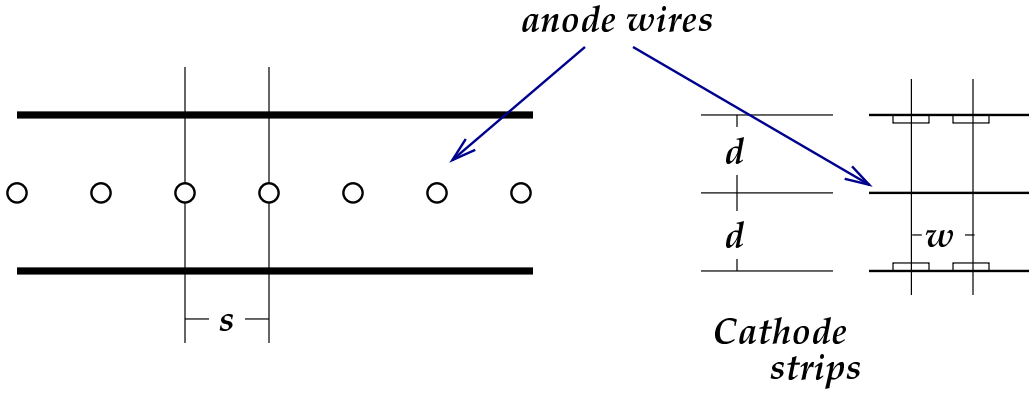

Figure 6: Schematic diagram of a generic cathode strip chamber defining the geometry described in the text.

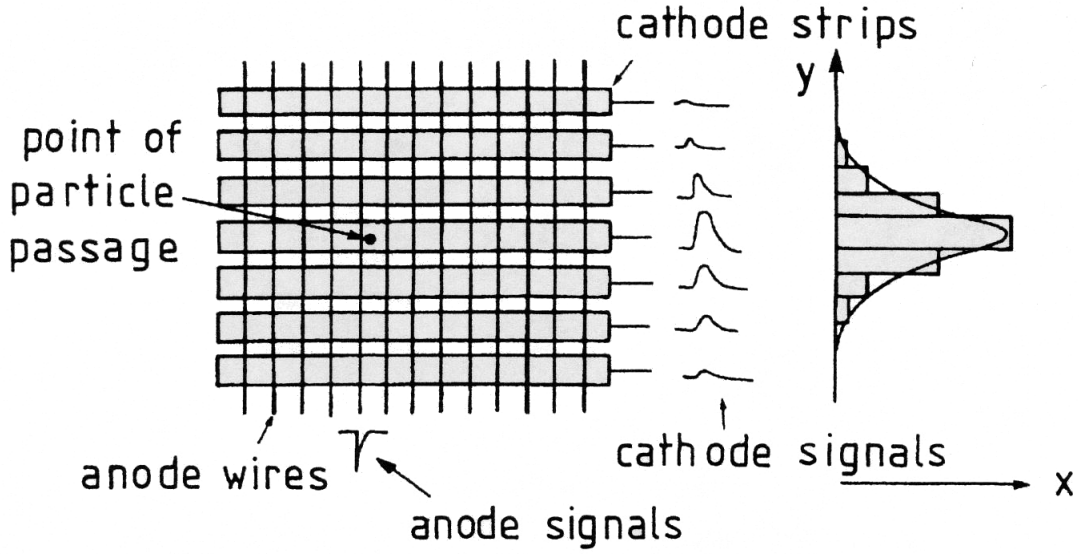

Figure 7: Illustration of the cathode readout in a typical MWPC.

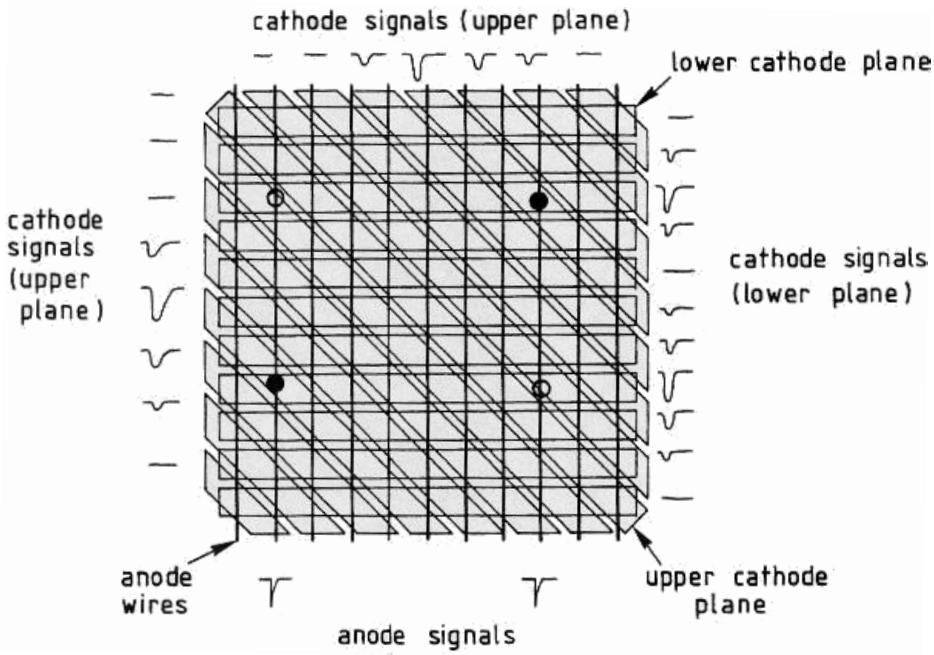

Figure 8: Illustration of the resolution of ambiguities within a CSC for two particle hits in a typical MWPC.

plane distortions should also be considered as well. The precision in the determination of the position of the induced charge depends linearly on the signal-to-noise ratio. Note that preamplifier noise is dominated by the input capacitance and that optimal capacitive coupling requires that the inter-strip capacitance be much larger than the capacitance of a strip to ground [7]. Operation within a realistic experimental environment will result in resolutions much closer to our design goal of 150–200 μm.

An interesting question regarding cathode chambers regards the change in system resolution when they are also employed as drift chambers (MWDCs), specifically horizontal drift chambers. The principles of operation of a MWDC are such that the best position resolution is achieved when the first electrons that reach the anode wire drift along field lines in the plane of the wires. If we consider a GARFIELD calculation [8] of the field lines for such a chamber (see Fig. 9(a)), the first electrons to reach the anode wire will most certainly arise from other locations within the drift cell. This gives rise to non-linearities in the space-time correlation that strongly degrade the position resolution, especially in a strong magnetic field. In order to improve the field configuration for the MWDC operation, field-shaping wires can be included within the anode plane between each anode wire. This can clearly improve the field configuration as shown in Fig. 9(b).

The basic algorithm to determine the cathode position of the charged track is to fit the charge distribution across the cathode plane. As an example, one algorithm to determine the position of the center of gravity is to use the ratio of the first and second moments of the charge distribution on the plane of the strips from [7]:

$$x_{c.g.} = \frac{\sum_{i=1}^{N} x_i q_i}{\sum_{i=1}^{N} q_i}, \tag{3}$$

where x_i=iw and w is the pitch of the cathode readout. If the charges q_i are measured with

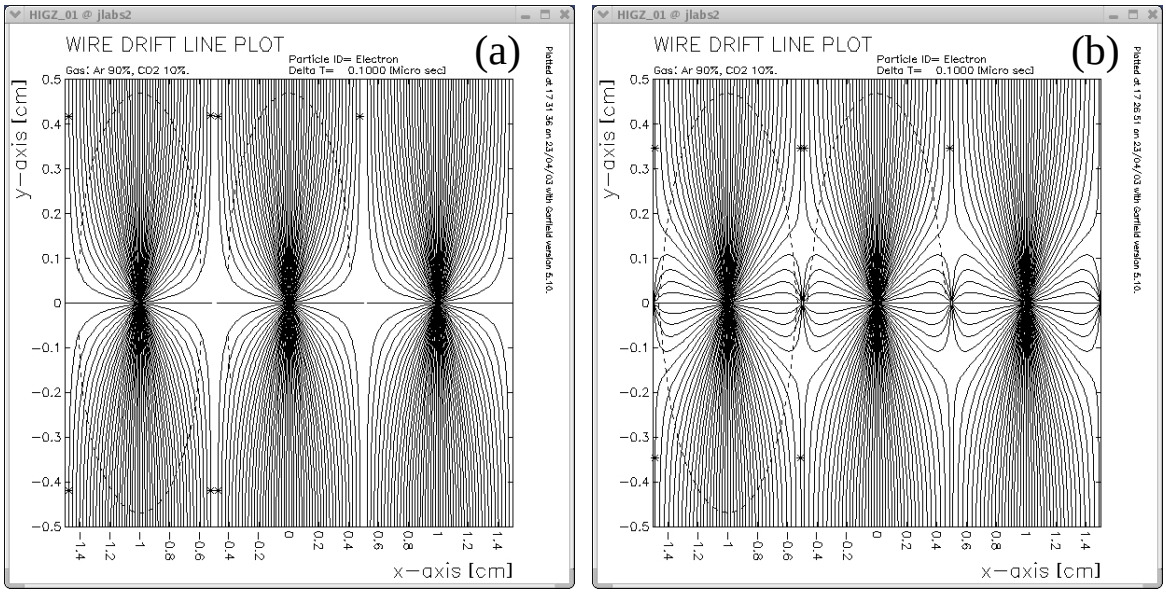

Figure 9: GARFIELD calculations of electric field lines (for a B=0 field configuration) within a square drift cell for a 90% argon - 10% CO_2 gas mixture for electrode configurations without (a) and with (b) field-shaping wires.

an RMS error of σ, then the uncertainty in $x_{c.g.}$ is given by:

$$\sigma_{c.g.} = \frac{\sigma}{Q}\sqrt{2\sum_i x_i^2} \tag{4}$$

or

$$\sigma_{c.g.} = \frac{\sigma}{Q}\sqrt{2w^2 + 2(4w^2) + 2(9w^2) + \ldots}\,. \tag{5}$$

Therefore the resolution depends on the number of strips used. Our Monte Carlo simulations and prototype studies, as well as operational experience from different groups have shown that the optimum number lies between three and five strips. The position resolution is poor when only one or two strips are present as there is not enough information, while it increases slowly when more than five strips are used. The resolution function in this case also includes the additional electronic noise from each strip. Here there must be an optimization of chamber resolution factoring in the desire to minimize the number of readout channels to contain costs. We have done extensive studies of several algorithms to extract a precision coordinate from the cathode plane information (see Ref. [9]). The c.g. form given above is just for illustration purposes.

One of the central questions that we have been investigating through our R&D program for the FDC system regards the optimal electrode structure in our cathode chambers. Specifically we are seeking to fully understand the trade-offs between timing resolution from the wire planes and spatial resolution from the cathode planes. The main question is how the inclusion of field-shaping wires affects the cathode position resolution. The results from our prototype studies, indicate that we can meet the design specifications for resolution in cath-

ode coordinates with the inclusion of the field wires. This is a novel aspect of our chamber design.

3 Small-Scale FDC Prototype Chamber

The FDC prototype cathode chamber has been designed primarily to provide us experience with cathode strip chambers. Through detailed study of this prototype we have been able to make design decisions on which electrode structure and layout will fulfill the design requirements for the final FDC chambers. The prototype has also provided important insights into the mechanical design, tolerances, construction and assembly techniques, noise immunity, and calibrations that will be important for the final FDC detector design. Some of the elements of the FDC prototype design have descended from the cathode chambers employed in the original LASS spectrometer [10].

A schematic of the FDC prototype chamber is shown in an exploded view in Fig. 10. The basic chamber layout consists of two cathode planes with strips oriented at $\pm 45^\circ$ sandwiching a single wire plane. The gas volume is defined by two outer aluminum frames that each include an aluminized mylar window. The active area of the prototype chamber is roughly 20 cm $\times$ 20 cm, and the chamber is about 8 cm thick.

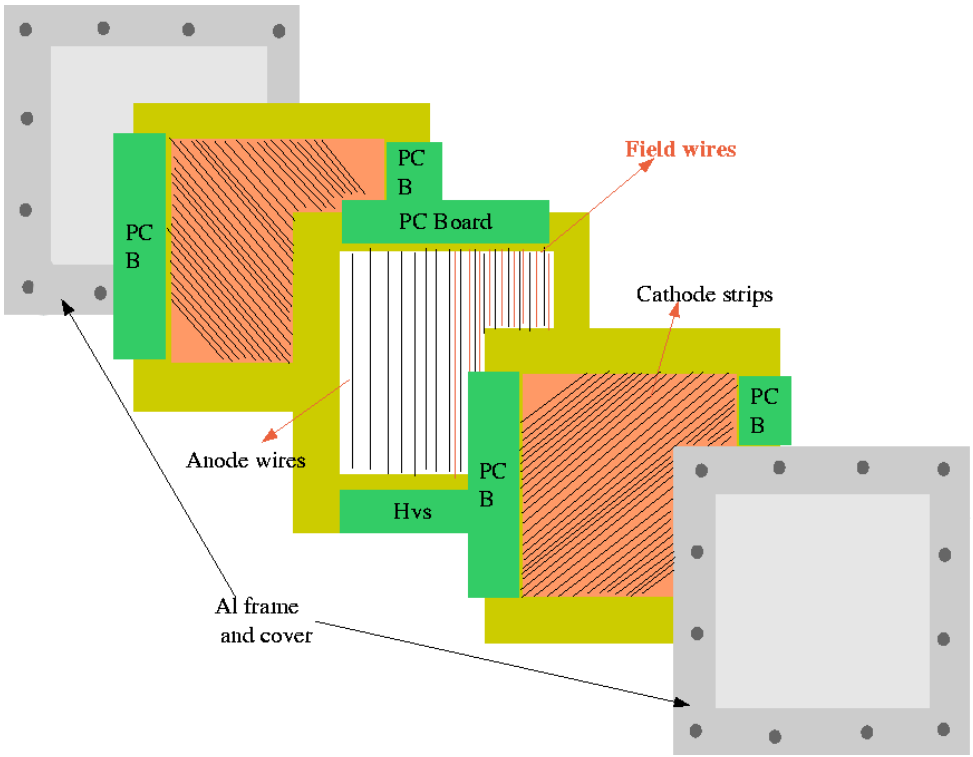

Figure 10: Schematic representation of the FDC prototype chamber in an exploded view showing the wire plane, two cathode planes, and the two aluminum window frames.

The test chamber has purposefully been designed to act as a test bed for any number of electrode configurations. So far we have tested wire planes consisting only of anode wires and

planes consisting of alternating anode and field-shaping wires. We have also designed cathode planes of varying rotation angle and varying cathode strip separations. Each configuration has been studied in order to come to an understanding of the optimal electrode structure for our purposes.

The U and V cathode planes are mirror symmetric with respect to each other. The cathode planes are copper-clad Kapton sheets ($\sim$2 mil thickness) mounted onto 5-mm thick G10 frames. The chamber is designed to operate with the anode wires at positive high voltage, the field wires at negative high voltage, and the cathode strips at ground.

The printed circuit board for the wires was designed to capacitively decouple high voltage from the signals and to route the signals to the output connector. The printed circuit board for the cathodes routes the signals directly to the output connector. The basic circuits on the boards are shown in Fig. 11. Small signal routing circuit boards attach to the output connectors on the wire and cathode circuit boards, and contain the preamplifiers for each readout channel. The output connects to a shielded twisted-pair line that routes the signals to the readout electronics. The signal readout boards used for the cathode readout are different than those for the wire readout in order to account for the polarity difference in these signals.

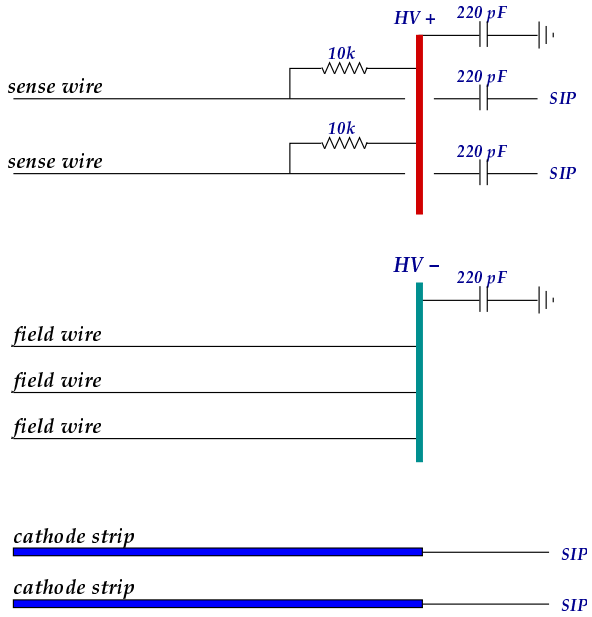

Figure 11: Circuit board electronics for the sense and field wires, along with the cathode strips.

Each readout channel has its own associated "SIP" preamplifier. These single-channel transimpedance preamplifiers were originally designed for the Hall B CLAS detector. They have complementary outputs designed to amplify signals by a factor of 2.25 mV/μA. Besides high gain, characteristics of the SIPs include: fast rise and fall times (3 to 4 ns), wide frequency bandwidth, wide dynamic range, and low noise and power dissipation (65 mW). The power requirement for a single SIP is 5 VDC at 13 mA, and is supplied by a low-voltage power supply.

In total the chamber includes 16 sense wires, separated by 1 cm. The cathode planes

are located 5 mm away from the wire plane. They each include 32 copper strips with a pitch of 5 mm. Three different sets of U and V cathode planes have been designed with strip separations of 0.25 mm, 0.50 mm, and 0.75 mm to allow for the optimal configuration to be determined. Studies from the prototype chamber indicate no differences in cathode resolution or noise levels among the different configurations. Our nominal strip gap choice is 1 mm. Presently the chamber is operating with a 90% argon - 10% CO_2 gas mixture. Photographs of the prototype cathode chamber and the cathode plane itself are shown in Fig. 12.

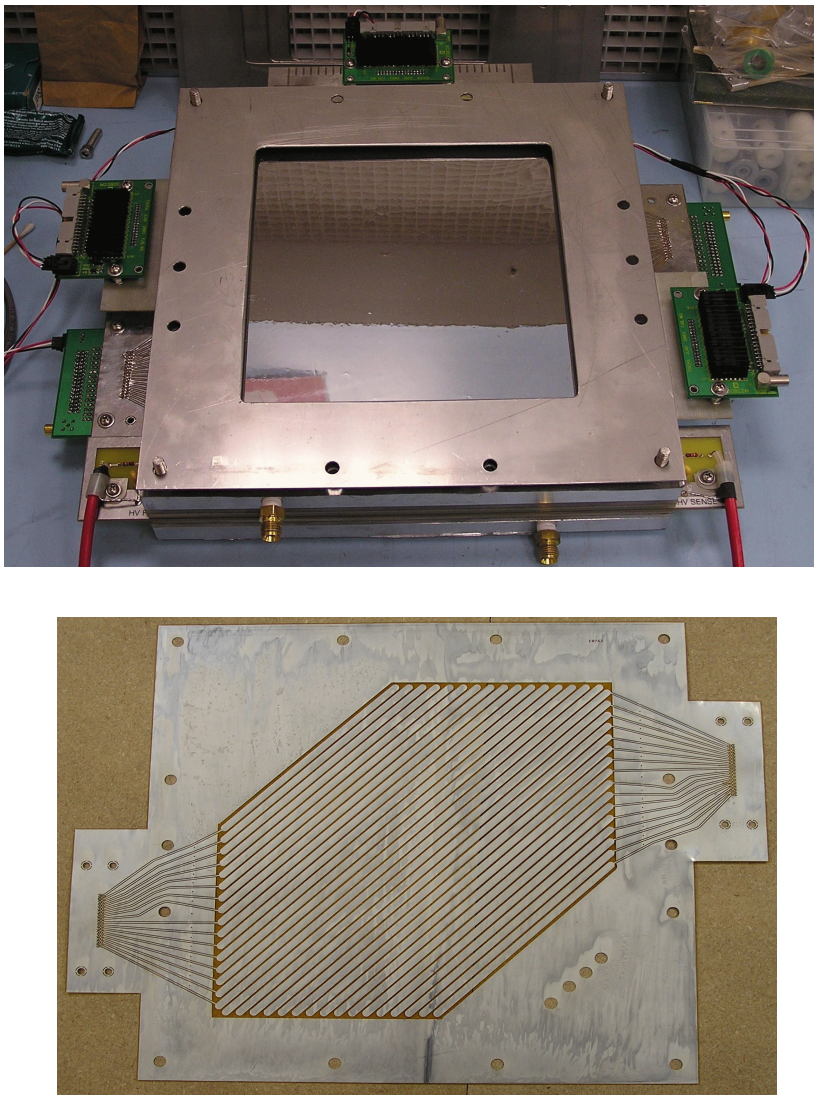

Figure 12: (Top) Photograph of the prototype FDC cathode chamber constructed to optimize the chamber structures. (Bottom) Photograph of a cathode plane showing the cathode strips.

A set of 19 wire chambers have been borrowed from IUCF in order to put together a cosmic ray test stand at Jefferson Laboratory. This test stand is being used to define tracks through the FDC prototype chamber. This system employs multiple layers of drift chambers above and below the FDC prototype chamber to precisely define the trajectory of

an incident charged particle track that can be used to compare against the position measured in the FDC prototype. This position difference represents a convolution of the resolution of the test stand and of the FDC prototype. The configuration of the test stand includes two X layers and two Y layers above the FDC prototype and a matching set of four layers below. This system is capable of defining a track to roughly 200 μm at the location of the FDC prototype. A photograph of the test setup is shown in Fig. 13.

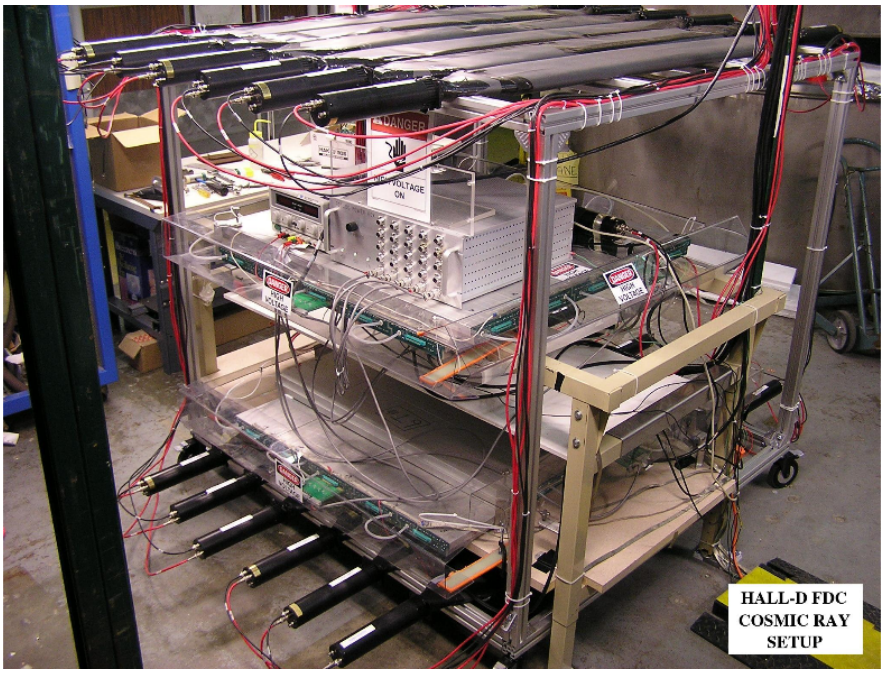

Figure 13: Photograph of the cosmic ray test stand set up at Jefferson Laboratory to study resolution characteristics of the FDC cathode strip chambers.

Fig. 14 shows the results of a GARFIELD calculation [8] of the electric field line and equipotentials for the case for our nominal electrode configuration where the high voltage on the sense and field wires is 1650 V and -300 V, respectively, the cathode planes are grounded, and the gas mixture in the chamber consists of a mixture of 90% argon and 10% carbon dioxide. This voltage setting was chosen to give an equal number of field lines from the anode wires terminating on both the cathode surface and the field wires in order to optimize the coordinate resolution from both the cathode strips and the drift time measurement. The field strength near the wires and the surface charge density for this configuration are listed in Table 1.

GARFIELD results for other high voltage combinations are described in Ref. [11]. Fig. 15 illustrates that the long-time edge of the drift time distribution is poorly defined when the field wires are absent but the distribution becomes sharper when the field wires are present, especially when the magnitude of the voltage on the field wires is increased. The effect of changing the field wire high voltage on the position resolution derived from the cathode strip data is described in Section 5.

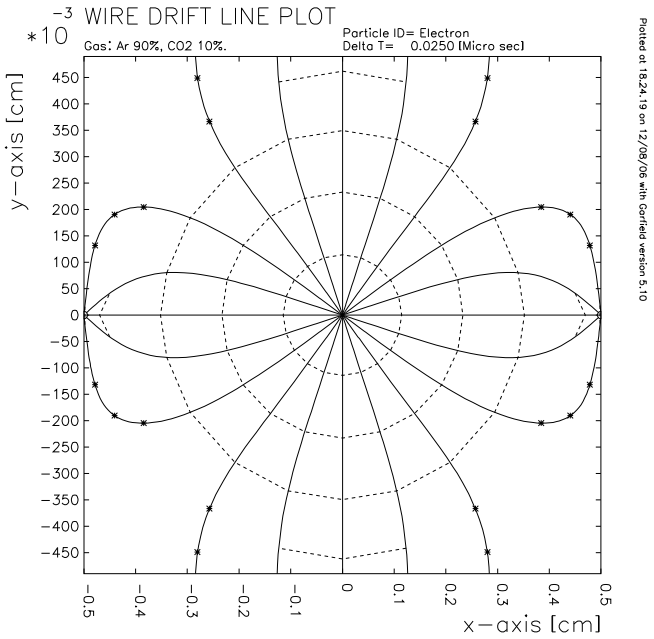

Figure 14: GARFIELD calculation result showing the electric field lines and equipotential contours for our nominal cell configuration at voltage settings of V_s=1650 V and V_f=-300 V.

	Charge	Surface field (kV/cm)	Field at $2r$ (kV/cm)	Surface pot. (volts)	Pot. at $2r$ (volts)
Sense wire	263.68	263.68	131.84	1650.0	1467.2
Field wire	-113.49	16.21	8.11	-300.0	-221.3

Table 1: Charge, surface electric field, electric field at twice the wire radius, surface potential, and potential at twice the wire radius for the wire plane with +1650 V on the sense wires and -300 V on the field wires.

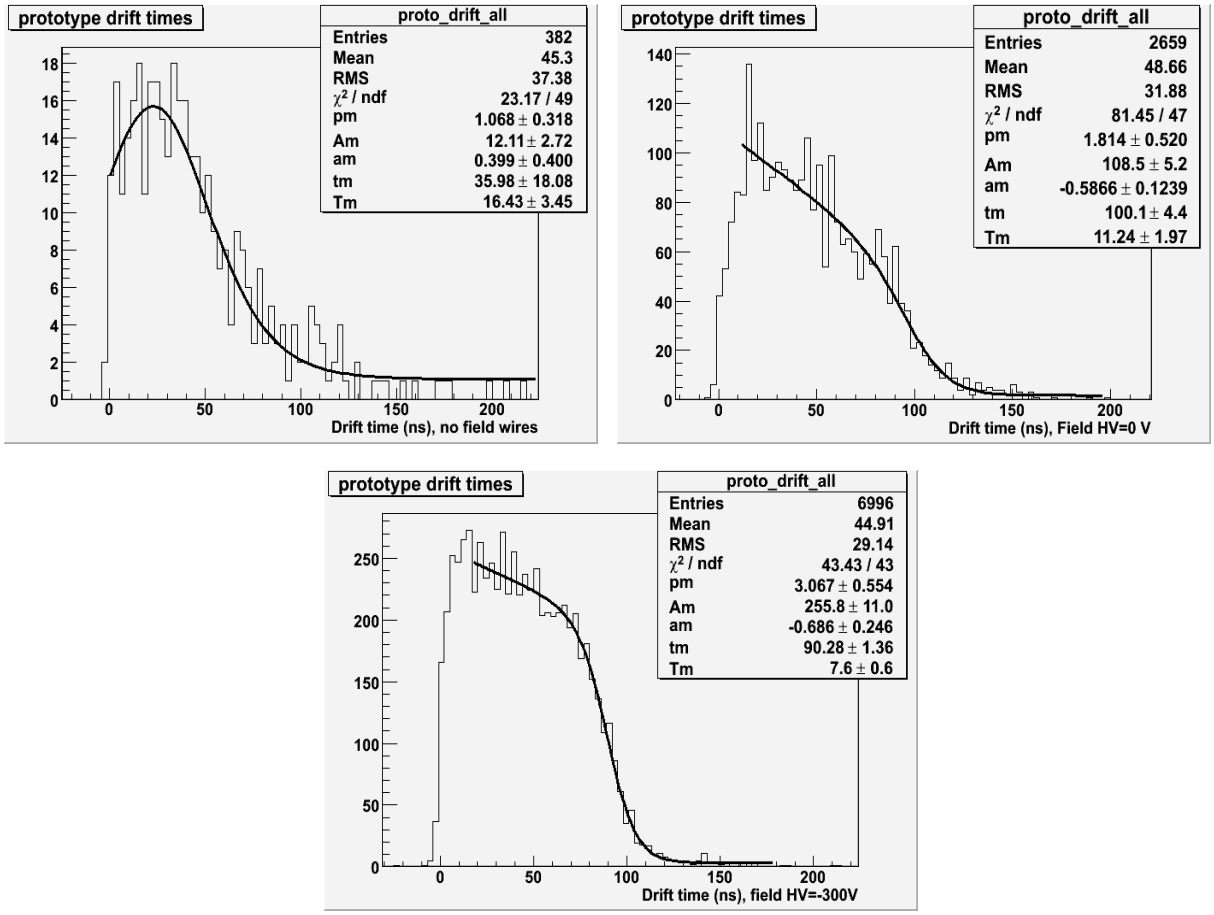

Figure 15: FDC prototype drift distributions for the sense wire only plane with the sense wires at +1750 V (top left), the field+sense wire plane with the field wires at zero potential and the sense wires at 1650 V, (top right), and the field+sense wire plane with the field wires at -300 V and the sense wires at 1650 V (bottom).

4 Anode-Cathode Separation

The gain of the FDC chambers depends critically on the separation between the cathode planes and the wire plane (referred to as the "half-gap"). Our early cathode plane samples suffered from noticeable folds and wrinkles that lead to local variations in the half-gap and hence the gain. In our small-scale prototype we did not attempt to pretension the cathode planes before they were attached to their frames to remove the defects. Thus the resolution measurements reported in this document should represent an upper limit from our design. We have been in contact with the circuit board manufacturers regarding the defects and they will able able to work with us to eliminate these problems. For the full-scale cathode planes our nominal flatness specifications for the cathodes are 50 μm.

Beyond local distortions in the cathode due to folds and wrinkles, there is another important distortion effect that must be considered in the design of the full-scale cathodes. When high voltage is applied to the wires, the grounded cathode planes are deflected toward the wires dues to electrostatic pressure as described in Ref. [12]. This distortion is largest at the center of the cathodes and uniformly decreases to zero at the perimeter. Kapton by itself offers little resistance to this deflection. In the small-scale prototype, given its small size, this deflection does not present a serious problem. We are currently investigating two techniques to mitigate this electrostatic distortion to optimize the chamber resolution. The first approach is to pretension the cathode planes and to attach the pretensioned planes to a support frame. The second approach is to laminate the cathode plane to a rigid backing. Both approaches, which are described further below, have advantages and disadvantages.

The effect of decreasing the half-gap on cathode signals was studied by the ATLAS group for a cathode strip chamber similar to our prototype. Fig. 16 shows the relative change of the cathode signals as a function of the change in the half-gap. Assuming these results can be generalized to our geometry, we have set a flatness goal of ± 50 μm, corresponding to a change in the cathode signals of $\pm 5\%$.

To illustrate the issue at hand, the gain $\mathcal{G}$ in a proportional counter is given in general by:

$$\mathcal{G} = Ke^{CV}. \tag{6}$$

For an operational voltage V, the gain is dependent on the capacitance of the detector C. Thus any variation on the flatness of the cathode plane changes the capacitance of the detector and hence the gain. It also creates field non-uniformities that affect the cathode position resolution. For gain variations of less than 5%, a rough calculation shows that the cathode plane must have less than a ± 5 mil flatness variation.

Various schemes have been employed by different groups to provide mechanical support for the cathode planes in large area chambers. For example, in the so-called *Plug Chambers* used in the LASS experiment [10], polyurethane spacers were epoxied onto the cathodes to fix the anode-cathode gap spacing. Our approaches, discussed below, have been designed to allow for the easiest and most robust system to establish and maintain the mechanical tolerances.

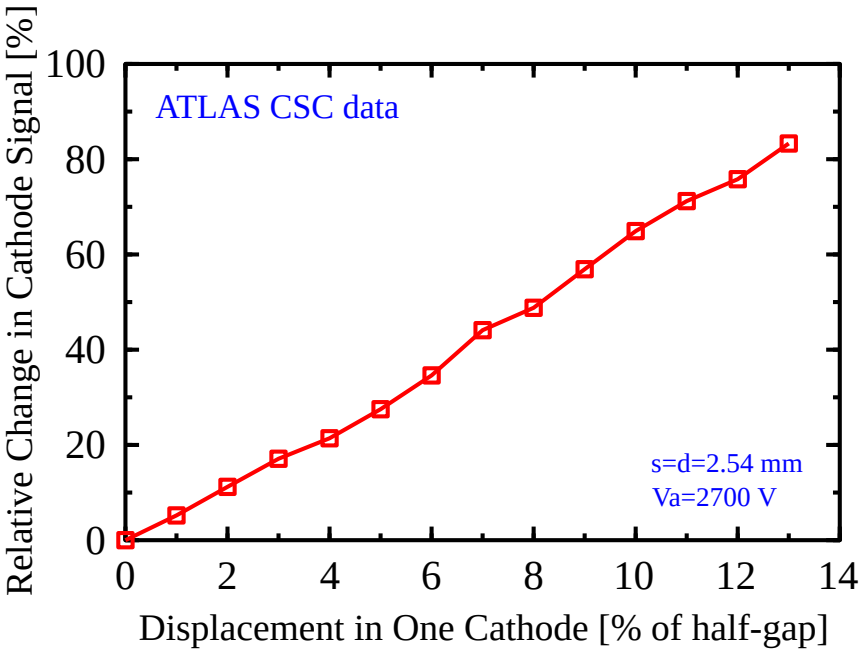

Figure 16: Cathode signal dependence on the half-gap from ATLAS CSC data. This figure is taken from Ref. [13].

4.1 Cathode Plane Tensioning

Our first approach in order to maintain the cathode plane flatness to our specifications is to pretension the cathode planes. This method has the advantage of reducing the amount of material within the detector, but suffers from the lateral distortions it induces on the cathode planes. Brian Kross of the JLab Detector Group has designed a tensioning mechanism for the cathode planes of the small-scale prototype. This system, illustrated in Fig. 17, is based on two concentric rings. The cathode plane (labeled "film" in the diagram) is epoxied face down to the top plate and pulled over the ridge in the bottom plate by using a set of screws at various places around the circumference of the top plate.

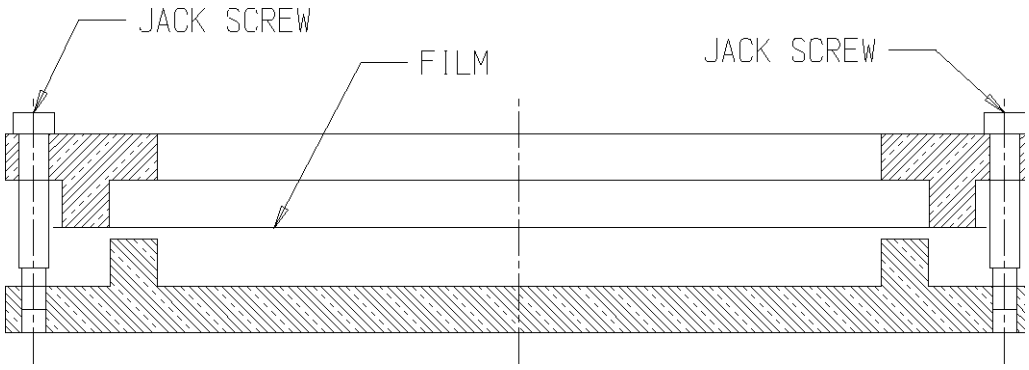

Figure 17: Side view of apparatus for tensioning the cathode planes.

A set of tensioned cathode planes was installed in the small-scale prototype. The tensioning was performed at a level to reduce the size of the folds and wrinkles to our predetermined flatness specifications. However the lateral distortions of the cathode strips in the tensioned planes were deemed unacceptable for the final detector design. In spite of this, we have installed a set of these tensioned planes in the small-scale prototype to compare against the untensioned planes. The final resolution results for the wrinkled planes were comparable to the tensioned planes (see Section 5).

Brian Kross has made adjustments to the design of the tensioning system given our experiences with the small-scale prototype cathode planes. The design of the tensioning system for the 1.2 m planes is complete and the parts have been ordered. We expect that a combination of improved quality of the cathode planes from the manufacturer coupled with improvements to the tensioning system will allow for a final decision to be made on this approach.

4.2 Cathode Plane Backing

Our second approach for establishing and maintaining the flatness of the 1.2 m cathode planes is to attach the Kapton planes to backing material made out of Rohacell, a very low density foam (ρ=0.032 g/cm^3). A sketch of the various components of a single layer of a package with this design is shown in Fig. 18. This approach is attractive in that the flatness tolerance for our cathodes can more easily be met without any worries of cathode plane lateral distortion. The drawback is the increased material thickness and the worsened momentum resolution. In this scheme we are working to include the backing while striving to minimize the overall material thickness.

To date we have obtained samples of the Rohacell foam and are studying its properties. Several groups at JLab have extensive experience with this material. It is used in Hall B to provide a backing for the mirrors in the Čerenkov counters being designed for the CLAS12 detector [14]. The material is fully machinable and its surface can be polished to a flatness well beneath those required for the FDC. Pieces of Rohacell that can be used for our 1.2 m cathode planes are now on order and a design has been completed to construct a cathode-Rohacell-ground plane-Rohacell-cathode "sandwich" using minimal epoxy layers. This will enable us to finalize our construction procedure for the full-scale prototype detector. We are also devising a scheme to quantify the flatness of the "sandwich". Based on these experiences, we will converge on a final design and a final set of quality control techniques.

We are also aggressively working to complete full GEANT Monte Carlo simulations of the FDC system to make final choices on the allowable material budget in order to achieve the design coordinate resolution values for the FDC. Our initial studies from a fast parametric Monte Carlo (HDFast) have indicated that our nominal sandwich design should allow us to achieve the design resolution for this system. We continue to hone the design to minimize the overall material thickness.

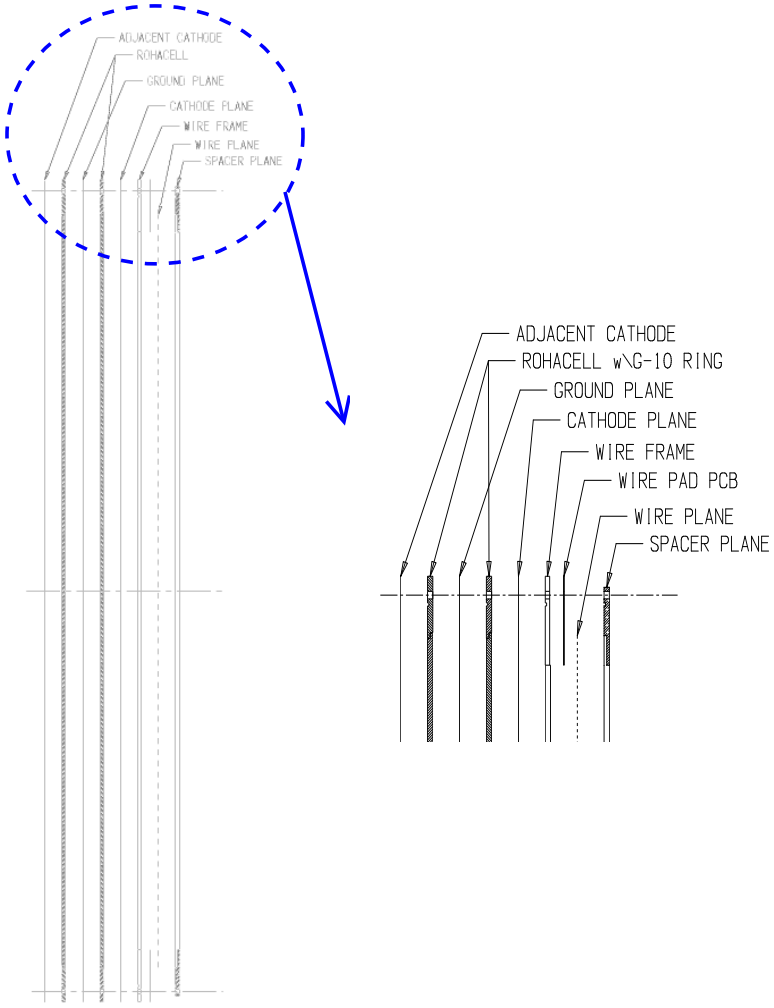

Figure 18: Sketch of the proposed structural components for one cathode-anode-cathode layer of the FDC. The structure repeats six times per FDC package.

5 Chamber Resolution Studies

This report presents the first results for the field+sense wire configuration of the anode plane. Fig. 19 shows the wire plane efficiency in a 90% argon - 10% CO_2 gas environment as a function of the voltage applied to the sense wires, with the field wires at zero potential. The efficiency is defined to be the ratio of the number of events that have one peak in each cathode view matched to a sense wire relative to the number of triggers. A narrow plateau occurs above about 1600 V. The setting we used for normal operation was 1650 V. Fig. 20 shows the anode charge (deduced from the cathode strip data) as a function of the sense wire high voltage. The trend is well-characterized by Sauli's gain function (eq.31 in Ref. [15]). Fig. 21 demonstrates that the position resolution improves with increasing sense wire voltage (and hence gain). It is not feasible to run the chamber with the sense wires at 1700 V because the wires start drawing too much current. However, with the sense wires set at 1650 V, the good resolution obtained at 1700 V can be recovered by increasing the magnitude of the voltage on the field wires, as demonstrated in Fig. 22. A plot of the wire positions reconstructed from the cathode data when the sense wires are at +1650 V and the field wires are at -300 V is shown in Fig. 23. The average position resolution under these conditions was 158.2 ± 3.1 μm. This improves upon the typical resolution of 182.6 μm obtained with the sense wire only configuration [9]. These studies indicate that the electrode structure of our nominal prototype design can achieve the required resolution for this tracking system. Additional results of these studies can also be found in Refs. [16, 17].

The cathode resolution as a function of x and y is shown in Fig. 24. Even with the relatively poor statistics in this study (acquired in a week–long run with incident cosmic ray muons), there is no indication of any strong dependence of cathode resolution on strip length. More detailed studies of the small-scale prototype are underway to better quantify the cathode resolution as a function of cathode strip length. In the full-scale chamber, the lengths of the cathode strips will vary from $\sim$10 cm to 1.2 m. The variation of the chamber resolution with strip length must be minimized.

The purpose of the cathode tensioning exercise was to make the planes as flat as possible and to minimize electrostatic deflections, thereby minimizing local variations in the gain that could in principle affect the resolution of the device. These tensioned planes replaced our original untensioned planes that suffered from numerous folds and wrinkles. Comparisons between the position resolutions obtained for the two configurations as a function of sense high voltage (Fig. 25) and field high voltage (Fig. 26) revealed no significant difference between the two sets of planes.

6 Monte Carlo Studies

The active area of the FDC will be limited by the requirement that the frames support the tension on the wires. A study using the Hall-D GEANT-based Monte Carlo, HD-GEANT, was performed to assess the effect on the acceptance of reducing the active radii of the FDC packages. Single muon tracks were thrown at all angles with respect to the direction of the beam with momenta in the range 0–9 GeV/c. To be accepted the primary track was required to create at least 8 hits in a tracking detector (FDC or CDC). Plots of the detector coverage

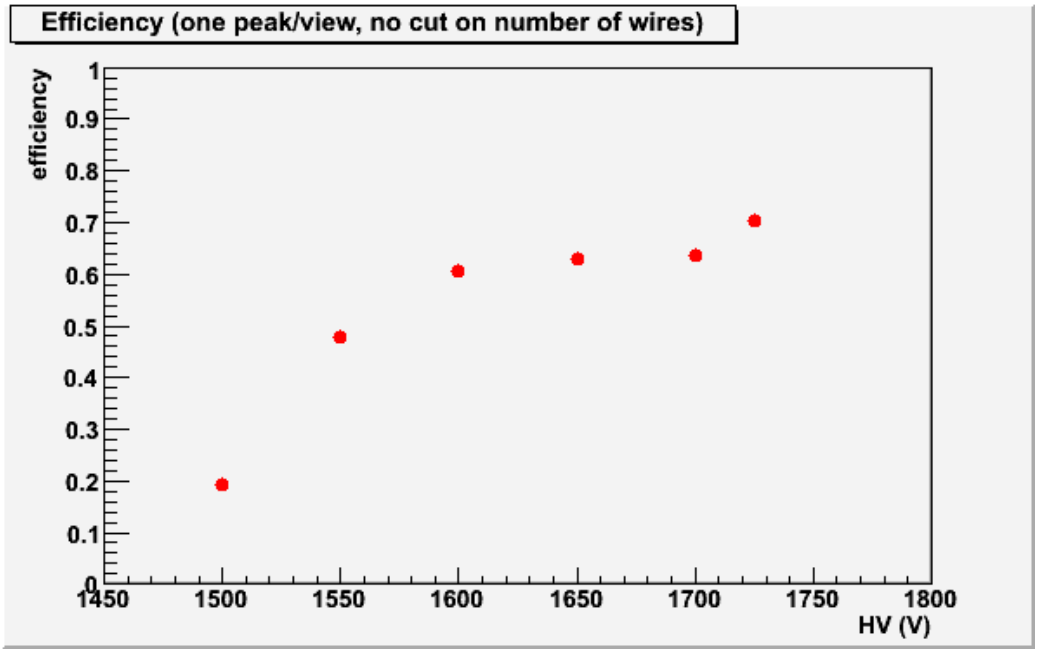

Figure 19: Efficiency as a function of sense wire high voltage for the field+sense wire configuration of the small prototype.

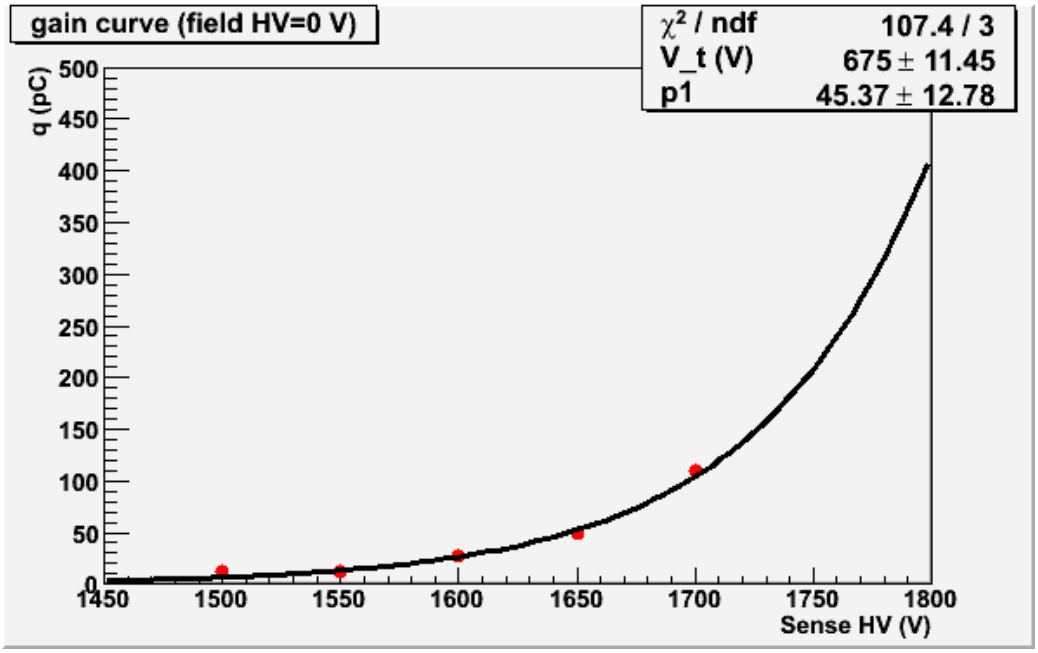

Figure 20: Chamber gain as a function of sense wire voltage with the field wires at zero potential.

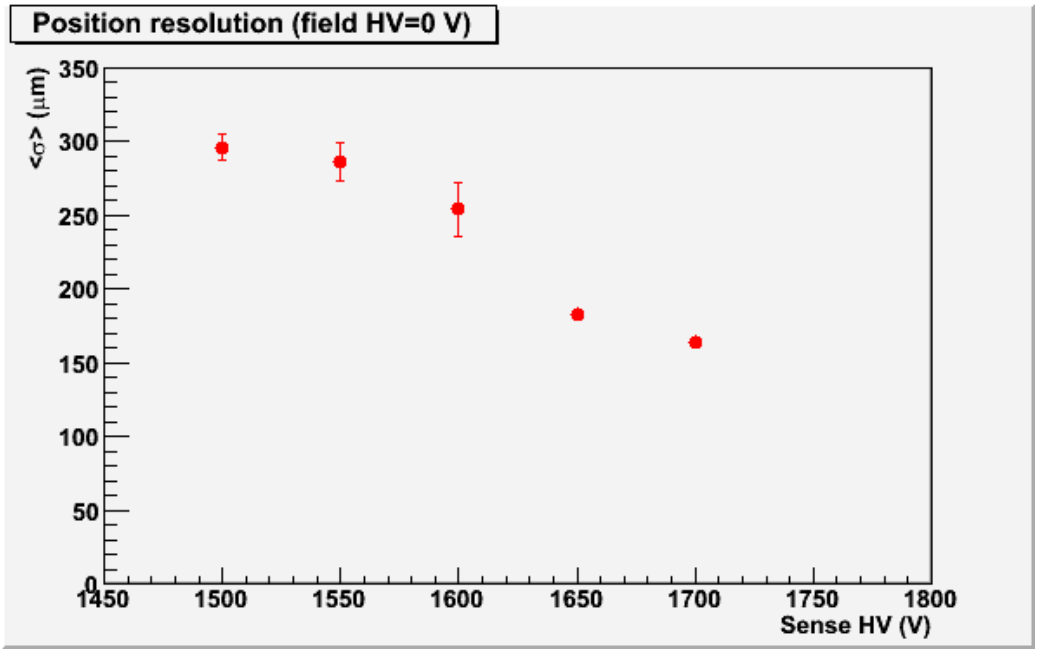

Figure 21: Position resolution as a function of sense wire voltage with the field wires at zero potential.

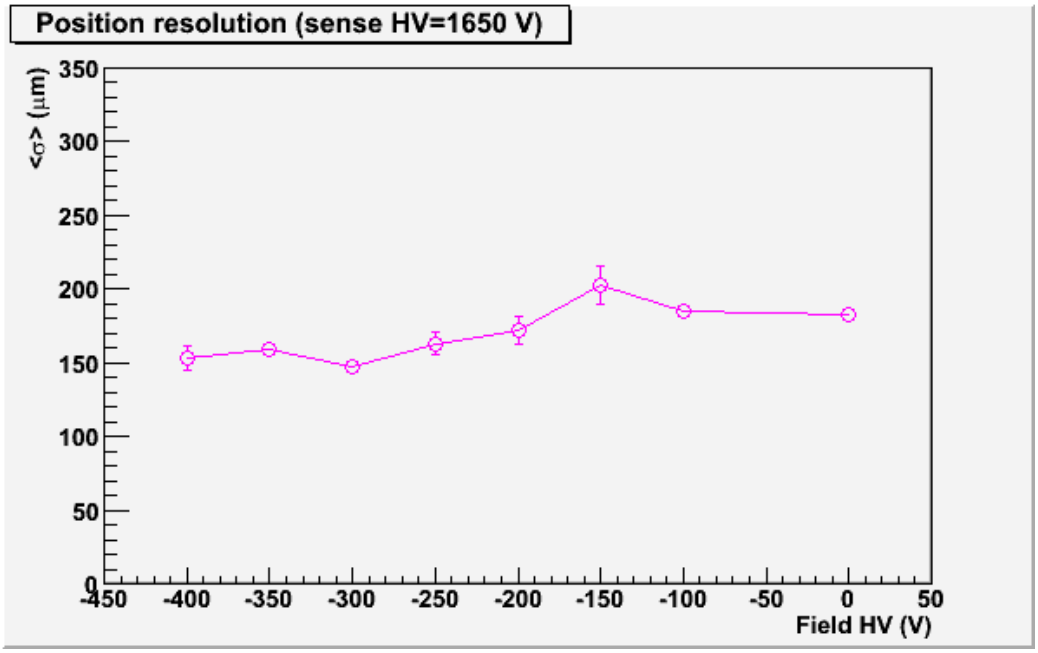

Figure 22: Position resolution as a function of field wire voltage with the sense wires at 1650 V.

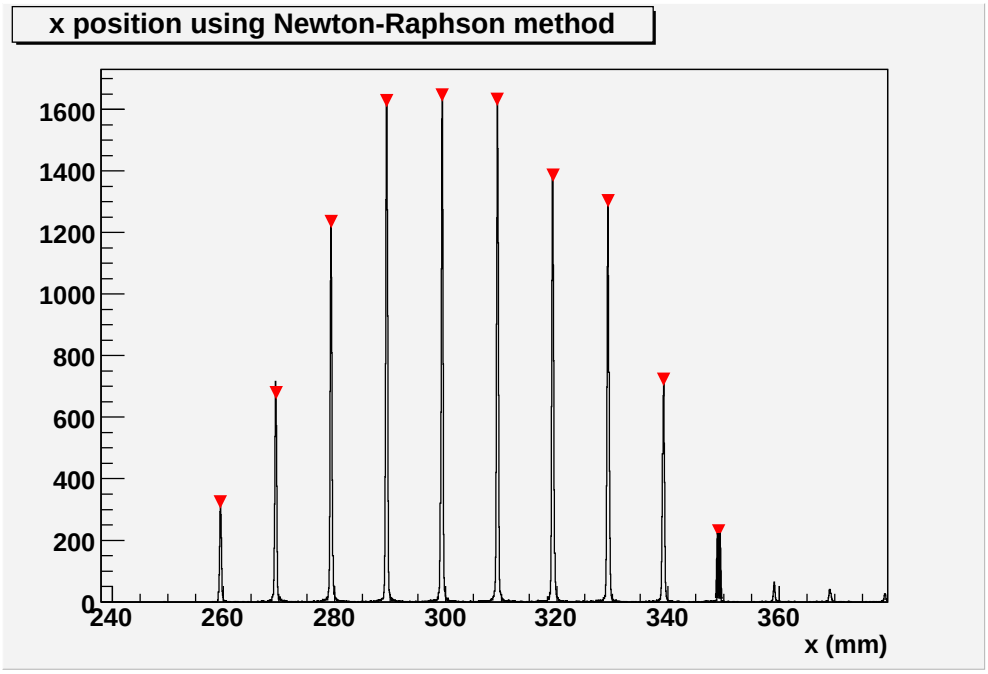

Figure 23: Wire position from cathode data for sense HV=1650 V, field HV=-300 V. The average cathode coordinate resolution from these data is 158.2±3.1 μm.

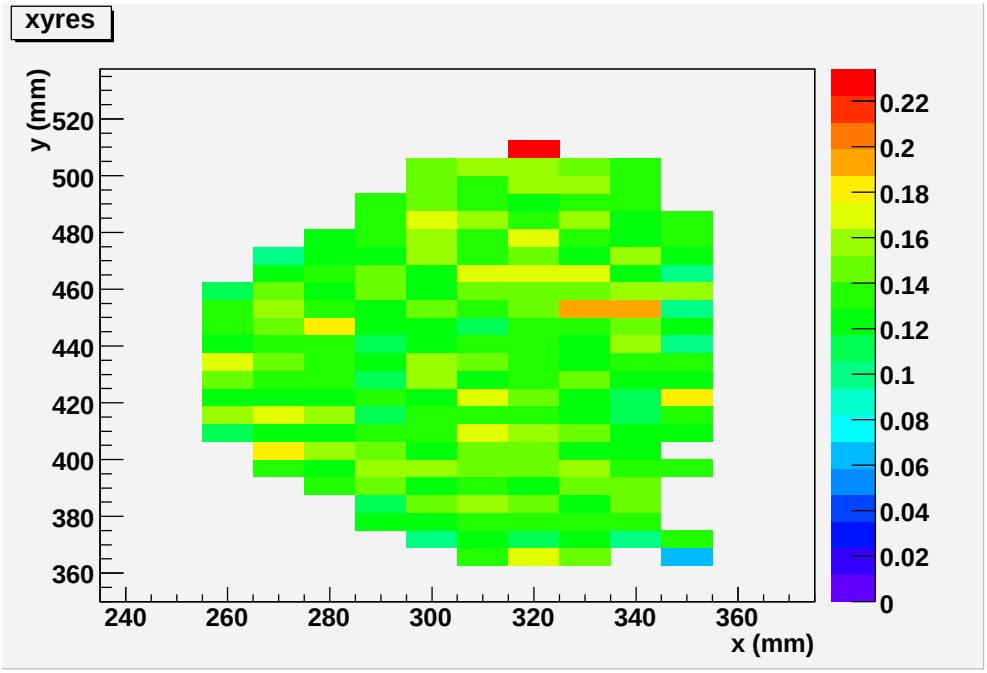

Figure 24: Position resolution as function of position for sense HV=1650 V, field HV=-300 V.

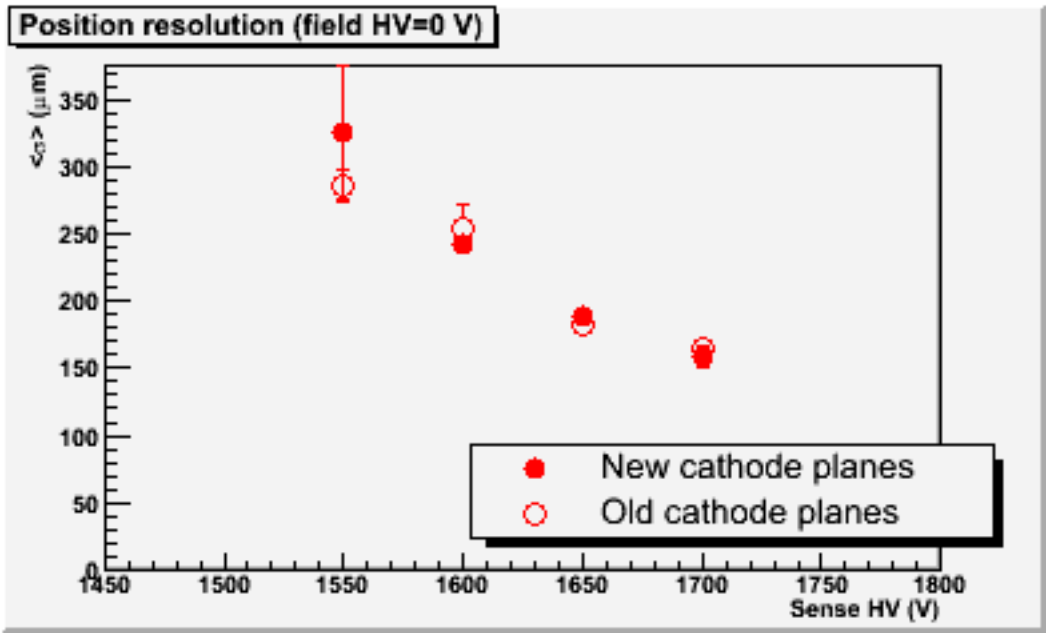

Figure 25: Comparison of position resolution as a function of sense wire high voltage (with the field wires at zero potential) between the tensioned cathode planes and the untensioned cathode planes.

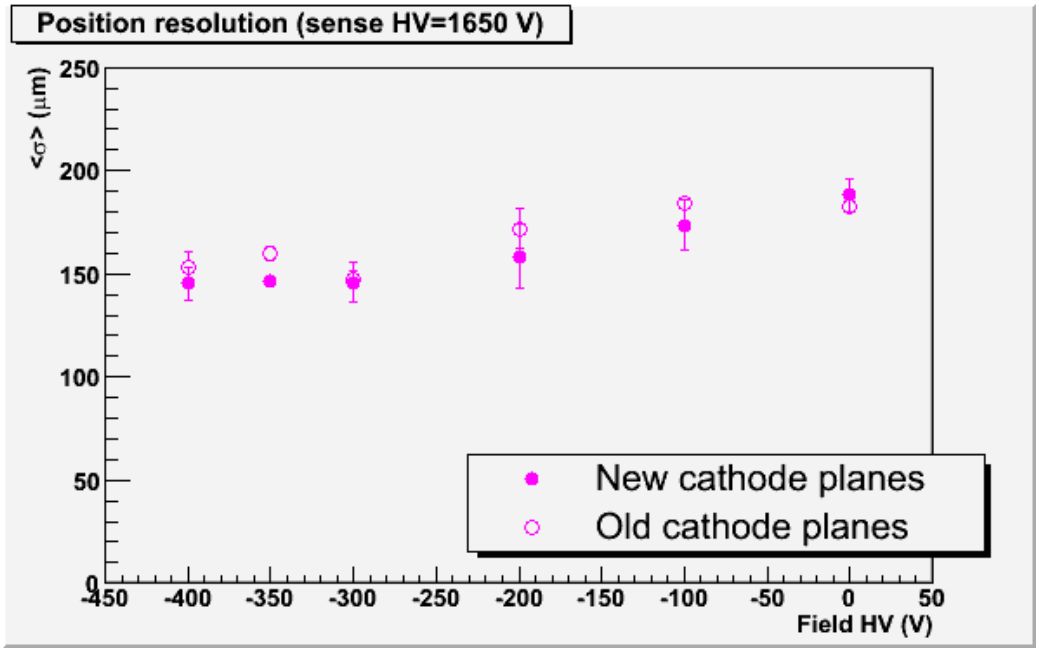

Figure 26: Comparison of position resolution as a function of field wire high voltage (with the sense wires at +1650 V) between the tensioned cathode planes and the untensioned cathode planes.

for several choices of the FDC outer radius are shown in Figs. 27 and 28. At an outer radius of about 49 cm and below, some events require hits in both the FDC and the CDC to be accepted because there is no longer an overlap between the two detectors. At an outer radius of 33 cm and below, holes in the acceptance start to appear.

The initial specifications for the layout of the FDC system have been studied within the framework of the HDFast Monte Carlo. The goals of the studies were twofold. First the basic number of FDC chamber packages within the solenoid was considered, as well as the number of drift chamber layers within each package. Secondly, the effect of the CDC design, specifically the 1-cm thick downstream endplate, was considered in its impact upon the resolution. For these studies, pions with momenta between 0.25 and 4.0 GeV were generated and the momentum uncertainty in the form of $\delta P/P$ was studied as a function of momentum. Fig. 29(a) shows a typical result comparing a 3-package vs. a 4-package configuration (with packages equally spaced along the beam line). Here the preliminary results make it apparent that the single track resolution, if all cathode and anode positions can be resolved to 150 μm, has improved resolution with the 4-package configuration. Although the resolution decreases with increasing momentum, the resolution of the 4-package configuration worsens at a slower rate than the 3-package configuration. The tracking system design parameters can be met with such a 4-package configuration. However, it is the redundancy that the fourth package provides that will be crucial in disentangling multiple charged particle hits and background within the readout time window. Monte Carlo studies for the number of measurements (i.e. wire planes) within a single FDC package are continuing in order to optimize the design. Preliminary studies however indicate that the 6-plane design is sufficient to meet the momentum resolution requirements for the tracking system. Further information on these studies in provided in Refs. [18, 19].

Fig. 29(b) shows a comparison of the Monte Carlo results with and without the 1-cm thick CDC endplate in position. For the simulation, the endplate was aluminum, however the current design plans are based on employing the polymer Delrin. The studies show that the resolution of the FDC system is worsened by roughly 10-15% due to the presence of the endplate.

At the present time the Monte Carlo work is proceeding in earnest to perform detailed systematic studies of the FDC design with realistic backgrounds in the chambers. This will enable final decisions to be made regarding the number of chamber packages, the number of anode planes, the optimal rotation between neighboring planes, and the optimal z-positions of the chambers.

7 Other Aspects of Full-Scale Prototype

There are several other aspects regarding the design and construction of the full-scale FDC prototype that deserve mention here. First the design of the circuit boards for the wire planes is now underway. This design has no technical challenges of note as this layout will follow standard practices in layouts of this sort. Brian Kross, Simon Taylor, and Daniel Carman will complete the initial design of this board. Final drawings and checks will be performed by Chris Cuevas of the JLab Electronics Design Group. Second, we have reached a tentative agreement with Karen Kephart at Fermilab to wind the wire planes for the detector. We will

Legend	
	Kinematical regime covered by CDC only
	Kinematical regime where 8 hits can be obtained from the CDC alone, but the FDC also has some acceptence.
	Kinematical regime where 8 hits can be obtained from either the CDC or the FDC. This is the area where there is the greatest overlap between the CDC and FDC.
	Kinematical regime where 8 hits can be obtained from the FDC alone, but the CDC also has some acceptence.
	Kinematical regime covered by FDC only
	Kinematical regime where hits from **both** the CDC and the FDC are required in order to get at least 8 hits.
	Little or no acceptance

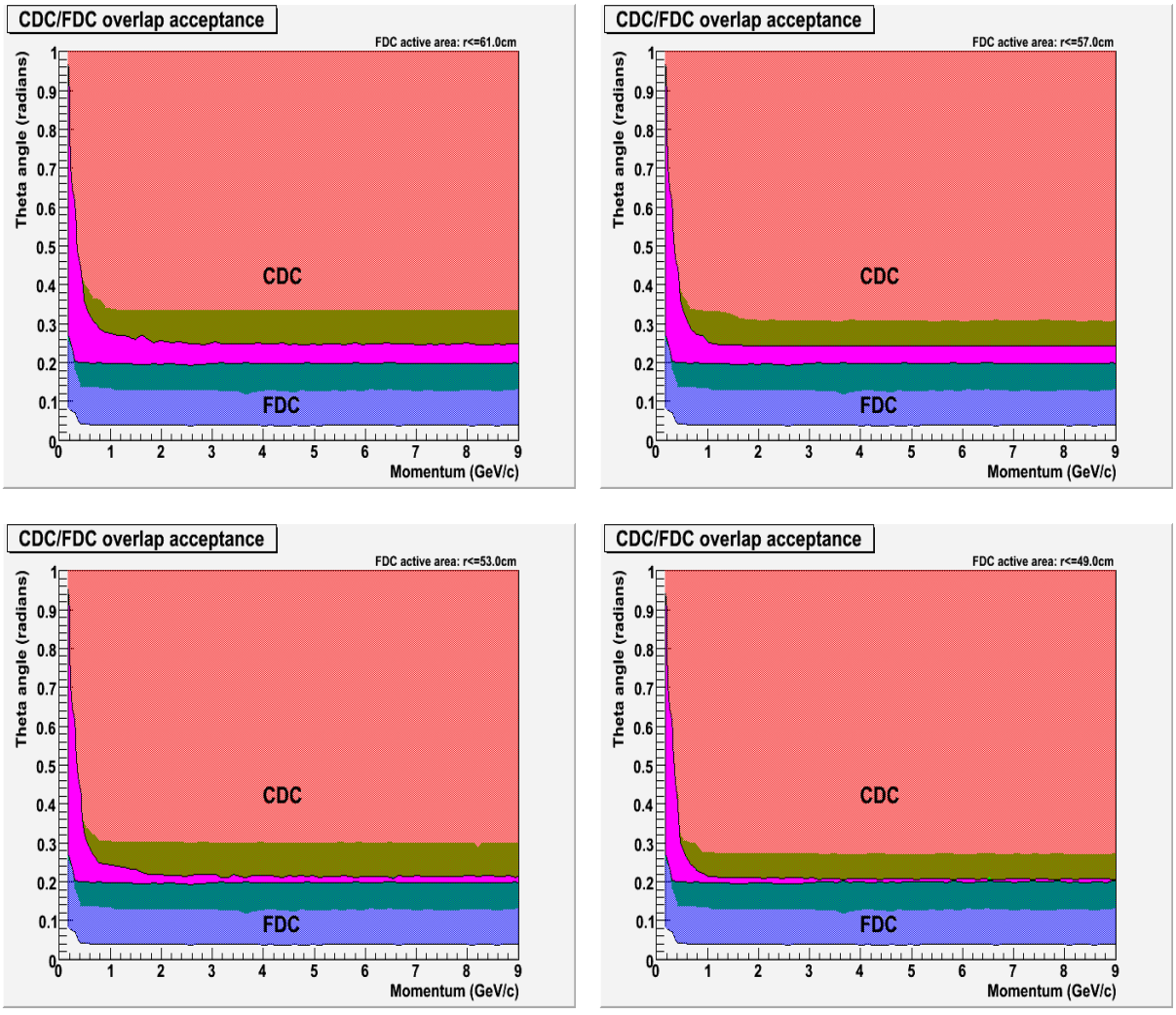

Figure 27: Acceptance as function of momentum and angle for the FDC and CDC. FDC outer radii for left column from top to bottom: r=61 cm, r=53 cm; radii for right column: r=57 cm, r=49 cm.

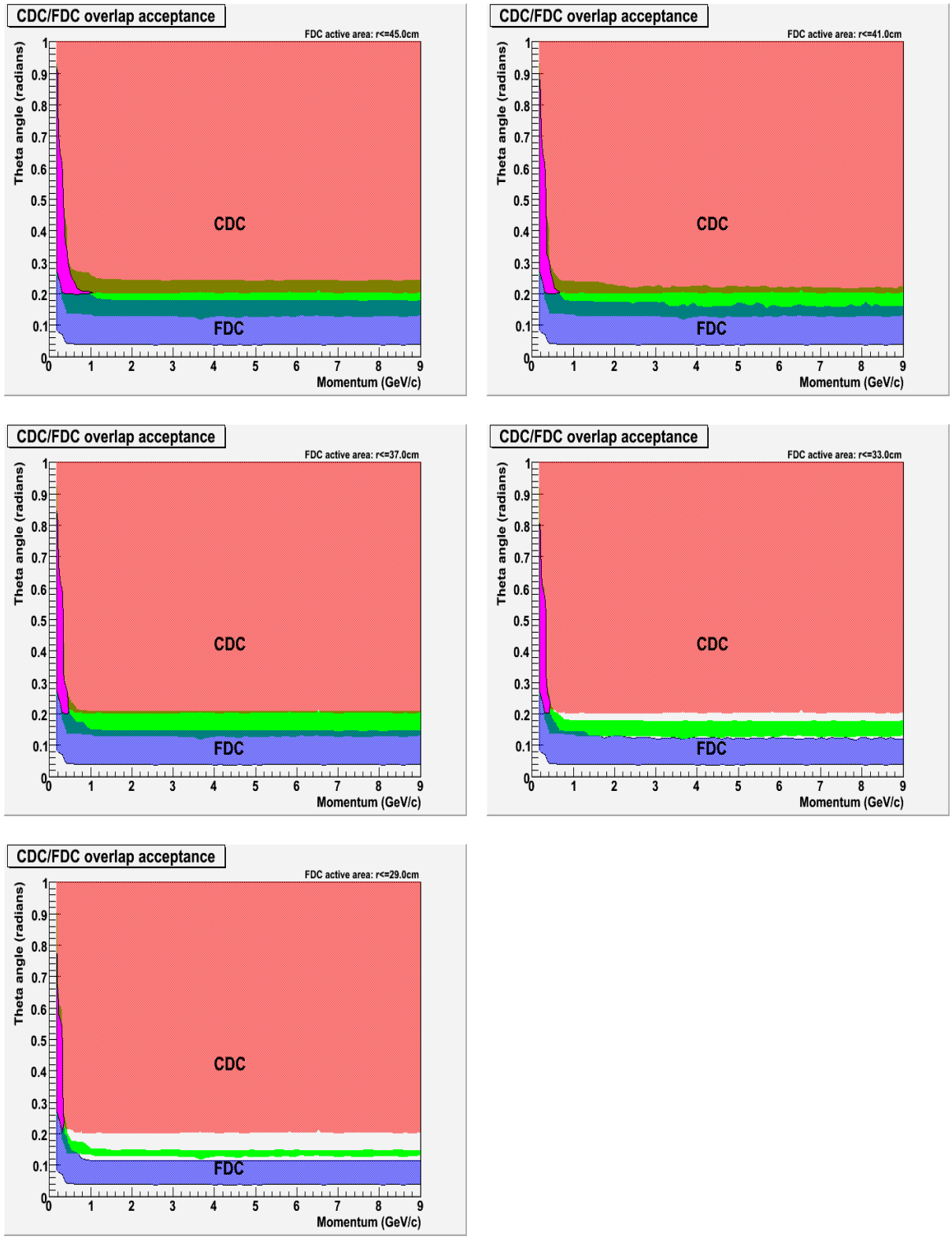

Figure 28: Continuation of Fig. 27. Left column from top to bottom: r=45 cm, r=37 cm, r=29 cm; right column from top to bottom: r=41 cm, r=33 cm.

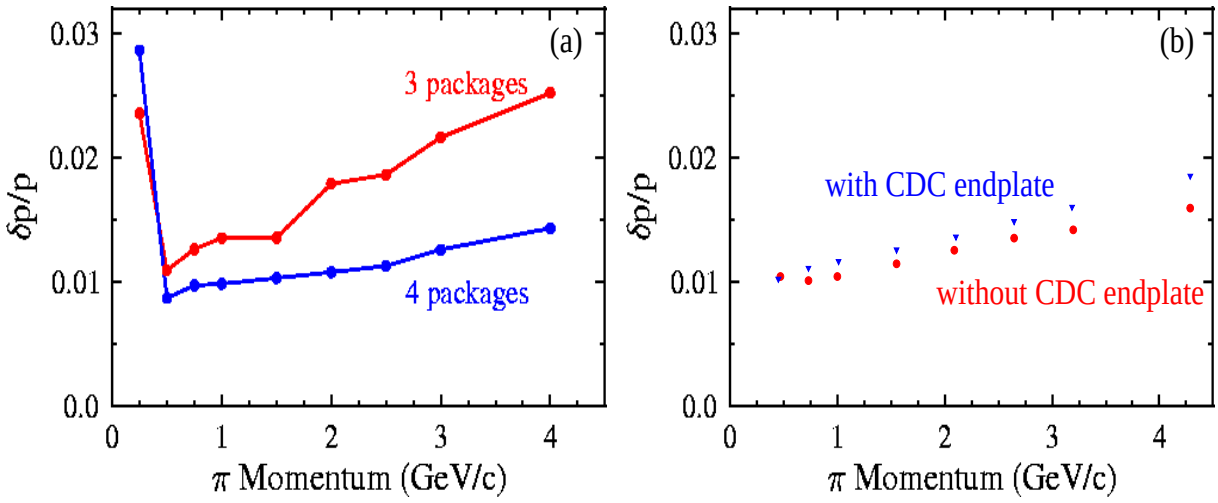

Figure 29: (a) Monte Carlo studies comparing the FDC resolution in a configuration with three packages vs. four packages. (b) Monte Carlo studies comparing the FDC resolution with and without a 1-cm thick aluminum CDC endplate.

also work with them to devise a scheme of quality control and wire placement measurements to ensure that the wire positions are within our design tolerances. Final checks and all remaining aspects of the detector assembly will be carried out by Daniel Carman, Simon Taylor, and Brian Kross.

8 Conclusions

Design and development studies for the full-scale FDC prototype chamber are underway. The design is based on lessons learned from the small-scale prototype cathode chamber that has been under study for nearly two years. In conjunction with these studies, we are also pursuing an R&D program with the detector group at JLab. We have identified the main areas of risk associated with the design of a cathode strip chamber and the mechanical constraints on the cathode planes. The design and techniques that are under study have shown that our approach is sound and that the resolution requirements for this system can be met. Our design for the chamber chamber and the electronics is based on the cathode chamber operating successfully in the ATLAS experiment at CERN. Our work has shown that the technical risks in the detector specifications are minimal and that the basic design of the full-scale prototype will be fully appropriate for the final design of the GlueX FDC system.

Appendix – Nominal FDC Design Parameters

Parameter	Value
Wire spacing s	10 mm (anode-anode) 5 mm (anode-field)
Anode-cathode distance, d	5.0 mm
Cathode readout pitch, w	5.0 mm
Gap between cathode strips, w_g	1.0 mm
Width of cathode strips	4.0 mm
Capacitance between strips	21 pF/m
Total strip capacitance	56 pF/m + 8 pF
Resistance between strips	$\sim$20 MΩ
Anode wire radius, r_a	0.010 mm
Wire capacitance per unit length, C_0	$\sim$9 pF/m
Gas gain	5×10^5
Operating voltage at nominal gain	1800 V
Electric field at cathode, E_c	<1 kV/cm
Electric field on anode wire surface	280 kV/cm
Field-shaping wire radius	0.040 mm
Electric field on field-shaping wire surface	15 kV/cm
Positive ion mobility, μ^+	1.3 cm^2/V/s
Total ion pairs	94/cm
Minimum wire tension	50 gm
Total charge collected	$\sim$15.5 pC
Charge collected in 30 ns (%)	$\sim$20%

References

[1] FDC homepage: http://www.jlab.org/Hall-D/detector/fdc/.

[2] J.A. Kadyk, Nucl. Inst. and Methods A **300**, 436 (1991).

[3] S.B. Christo and M.D. Mestayer, "Minimizing Cathode Emission in Drift Chambers", CLAS-Note 92-016, (1992).

[4] Karen Kephart (FNAL), private communication.

[5] *PHENIX Collaboration.* PHENIX Internal Note PN125.

[6] H. Fenker *et al.*, Nucl. Inst. and Meth. A **367**, 285 (1999).

[7] *ATLAS Collaboration.* ATLAS Technical Design Report, Chapter 6, June 1997.

[8] GARFIELD has been developed at the University of Mainz by R. Veenhof and revised by M. Guckes and K. Peters. See HELIOS-note 154, (1986).

[9] S. Taylor and D.S. Carman, *"Update on FDC Algorithm Development"*, GlueX-doc-601-v2.

[10] D. Aston *et al. (The LASS Collaboration).* SLAC Internal Note SLAC-298.

[11] D. S. Carman, "FDC Garfield Studies v1.0", (http://www.jlab.org/Hall-D/detector/fdc/design/garfield_study.ps).

[12] S. Taylor, *"Deflections of Cathode Planes Due to Electrostatic Pressure"*, GlueX-doc-668-v1.

[13] Figure taken from talk by Paul O'Connor.

[14] Y. Sharabian, private communication.

[15] F. Sauli, "Principles of Operation of Multiwire Proportional and Drift Chambers", CERN 77-09.

[16] S. Taylor and D.S. Carman, *"Update on Studies of the FDC Prototype and Test Stand Setup"*, GlueX-doc-526-v1.

[17] S. Taylor and D.S. Carman, *"FDC Prototype Studies"*, GlueX-doc-453-v1.

[18] S. Taylor, *"Further HDFast simulations of the FDC"*, GlueX-doc–514-v1.

[19] S. Taylor, *"HDFast Simulation Study of the FDC"*, GlueX-doc-418-v2.